

Effect of OCA Properties on Foldable AMOLED Panel with a Module Structure

Yali Liu¹, Yongzhen Jia², Zhengzhou Liu³, Di Wu³, Haoqun Li¹, Zhuo Zhang¹

¹Wuhan China Star Optoelectronics Semiconductor Display Technology Co., Ltd, Wuhan, 430078, China

²Shenzhen China Star Optoelectronics Technology Co., Ltd, Shenzhen, 518132, China

³State Key Laboratory of Materials Processing and Die & Mould Technology, Huazhong University of Science and Technology, Wuhan, 430074, China

Keywords: OLED display; Foldability; OCA

ABSTRACT

The main design goal of the foldable OLED display is to avoid the film stack failure caused by bending stress during repeated folding and unfolding. This paper models and simulates the structure of the foldable OLED screen module, and explores the visco-hyperelastic mechanical characteristics for optical clear adhesive, such as the factors of influence of hyperelastic modulus, viscoelastic parameters E_{∞} and Poisson's ratio.

1 INTRODUCTION

Recently, the importance of flexible display technology is increasing on a daily basis as a result of the sustainable development of personal intelligent device[1-3]. Several flexible AMOLED products are already on sale in the display market. But, These products have some defects, for instance, device peeling, visible wrinkles etc. In order to realize flexible display perfectly applied to the rollable or foldable device of next generation, it is necessary to research the effective application of Optically clear adhesives (OCA) materials in the flexible AMOLED module.

The structure of a module flexible AMOLED display can be divided into several parts: cover window, polarizer touchpad, panel film and backplane; Another important component Adhesives (OCAs) which can be used to bond cover windows, touch sensors and circular polarizers in a foldable OLED display (Figure 1). For a foldable display module, OCA changes the direction of film stress and minimizes strain on critical layers, which is defined multi-neutral layer phenomenon. For a foldable display module, it is also desirable to have an adhesive that there are no visible wrinkles or buckles in the display and the adhesive should allow device to quickly return to the unfolded position, when the device is unfolding. Additionally, the adhesive should have minimal creep to avoid flow and a subsequent change in thickness in response to the strains in the folded position, When the device is folded. Therefore, it is particularly important to research the essential properties of OCA in the flexible AMOLED module. In 2014, Yeh et al, firstly used the finite element method to simulate the stress of the foldable OLED module [17]. the simulation

model only established a layer of first-order solid elements, and the final result showed a large calculation error because of the shear self-locking effect. Therefore, the simulation results were difficult to analyze the stress transfer between the thin film devices, and it was impossible to react to the actual stress. Jia et al[10].posed a constitutive model which was presented to describe the nonlinear visco- hyperelastic behaviors for OCA and the flexible panel module was shown to have multiple neutral planes, due to the decoupling effect of the OCA, but he did not elaborate on the hyper-viscoelastic properties of OCA in the flexible AMOLED module .

Based on the current research, this paper explores the OCA constitutive the flexible AMOLED module to describe the visco-hyperelastic characteristics. The finite element method (FEM) is employed to simulate the stress distribution of the module bending process. After proving the importance of multiple neutral layers to modules and finds the major influence factor of OCA from the hyperelastic modulus, viscoelastic parameters E_{∞} , Poisson's ratio, then can suggest the reasonable stack structure. Finally, reasonable stack structures can be given to protect the available suggestions are given to optimize the flexible AMOLED display.

2 EXPERIMENT

A foldable display is laminated with numerous thin layers, which is defined a simplified 7-layer film stack (Table 1) without consideration of the detailed patterned layout and materials of the OLED devices. In the fully folded configuration, the space between the straight sections of the outer layer is 6 mm resulting in the bent section of the film stack forming an approximate semi-circle of a radius of 3 mm as shown in Fig. 1.. During the first second, the rigid body rotates counterclockwise around the reference point at 1.57 rad/s while moving leftwards at $(\pi/2-1)*r$ mm/s, and then stays for 300s. In-folding motion means that the front sides of the display are attached to each other, the observable face is the back of the display. Out-folding motion means that the back sides of the display are adhered to each other, and the outside can still visually see the imaging of the

display (see Fig. 1c). The simulation was performed using the ABAQUS finite element analysis package. Due to the large ratio of film stack panel width to its thickness, a 2-dimensional plane strain model was used

3 RESULTS

3.1 The effects of the OCA layer thickness

In this section, the first OCA layer is adjusted. The thickness of the original first OCA layer is 25 μm. When investigating the influence of the thickness of the first OCA layer, the thickness of 25 μm, 50 μm, 75 μm, 100 μm, 125 μm is selected for comparison. We discuss the strain distribution at the symmetry axis and the maximum strain of each OCA layer after the model bent, and the results are shown in Fig 3-1(a) and Figure 3-1(b).

With the increase of the thickness of OCA1 adhesive layer, the maximum strain of each film layer does not change; The maximum strain of OCA1 layer decreases significantly, and the strain of OCA2 layer also decreases significantly. The strain of other OCA layers tends to decreasing, but not obviously.

3.2 The effect of hyperelasticity of the OCA material

The hyperelasticity of the OCA material is mainly reflected in the change of the elastic modulus with time. In this section, the experimental data of the OCA material is modified in proportion to achieve the change of the elastic modulus. The fitting parameters are shown in Table 1.

After calculating, the strain distribution at the axis of symmetry and the maximum strain of each OCA layer after bending are shown in Fig 3-2(a) and Fig 3-2(b).

With the increase of the elastic modulus, the strain curve of the display area is obviously shifted to the right, and the tensile strain is significantly increased. When the elastic modulus is increased to 1400 times, the strain neutral layer phenomenon disappears. When it increases to 140,000 times, the strain distribution is linear, the strain of each film layer is greatly increased, and the risk of damage of the device is increased. At the same time, the strain of each OCA layer is also significantly decreased.

3.3 The effect of viscoelasticity of the OCA material

The Prony series used to describe the viscoelastic behavior can be represented by the formula, which is equivalent to:

$$G(t) = G_0 \left(g_\infty + \sum_{i=1}^N g_i e^{-\frac{t}{\tau_i}} \right) \quad (3.3.1)$$

In the formula, g_∞ is e_∞ and g_i is the curve coefficient, satisfying:

$$g_\infty + \sum_{i=1}^N g_i = 1 \quad (3.3.2)$$

When changing g_∞ , other coefficients g_i can be obtained according to the ratio:

$$g_i = g_{0i} (1 - g_\infty) / (1 - g_{0\infty}) \quad (3.3.3)$$

In (1.3.3), g_{0i} , $g_{0\infty}$ are the Prony coefficients obtained by fitting the original data.

The Prony parameter τ_i remains unchanged when E_∞ changes. The Prony parameter corresponding to

different E_∞ is shown in Table 2. Using parameters to fit, the viscoelastic curve is obtained as shown in Figure 1-3. The larger the value of E_∞ , the closer the material is to elasticity. When $E_\infty = 1$, the material loses viscoelasticity and only has hyperelasticity.

It can be seen that the change of the viscoelastic parameters E_∞ does not cause an apparent change in the strain of the film. The strain of each layer is basically the same at 0 s after bending. However, the maximum strain of the layer at 300 s after bending, there have been changes, The fourth layer of OCA maximum strain grows 28.6%.

It indicates that the parameter E_∞ affects the material relaxation and creep properties, which affects the deformation of the material. When the E_∞ is larger, the viscoelastic property is less obvious. When the same time is left, the degree of deformation of the OCA material is more small.

4 DISCUSSION

A constitutive model was presented to describe the nonlinear viscohyperelastic behaviors for OCA. Based on the mechanical model, the stress and strain distribution of the flexible AMOLED touch panel in the folding state were analyzed by the finite element method. The folding symmetry, which is matched to the smallest curvature radius, bears the maximum stress. The curvature radius gets larger as the position is further away from the symmetry center. The stress can be decreased to nearly zero in the unbending area. (to be added)

5 CONCLUSIONS

As the thickness of the first OCA layer from 25 μm to 50 μm, the relative difference in OCA maximum strain of down to 37.5%. With the increase of the elastic modulus, the strain curve of the display area is obviously shifted to the right, and the tensile strain is significantly increased. When the E_∞ is larger, the viscoelastic property is less obvious. When the same time is left, the degree of deformation of the OCA material is more small.

REFERENCES

- [1] Niu Y F, Liu S F, Chiou J Y, et al. Improving the flexibility of AMOLED display through modulating thickness of layer stack structure[J]. Journal of the Society for Information Display, 2016, 24(5): 293-298.
- [2] Shi Y, Rogers J A, Gao C, et al. Multiple neutral axes in bending of a multiple-layer beam with extremely different elastic properties[J]. Journal of Applied Mechanics, 2014, 81(11): 114501.
- [3] Y.F. Niu, S.F. Liu, J.Y. Chiou, C.Y. Huang, Y.W. Chiu, M.H. Lai, Y.W. Liu, Improving the flexibility of AMOLED display through modulating thickness of layer stack structure, J. Soc. Inf. Disp. 24 (5) (2016) 293–298 <https://doi.org/10.1002/jsid.443>.

- [4] M.K. Yeh, L.Y. Chang, H.C. Cheng, P.H. Wang, Bending stress analysis of laminated foldable touch panel, *Procedia Eng* 79 (3) (2014) 189–193 <https://doi.org/10.1016/j.proeng.2014.06.330>.
- [5] Y. Shi, J.A. Rogers, C. Gao, Y. Huang, Multiphase neutral axis bending of a multiple layer beam with extremely different elastic properties, *J. Appl. Mech.* 81(11)(2016)114501 <https://doi.org/10.1115/1.4028465>.
- [6] C.C. Lee, J.C. Ho, G. Chen, M.H. Yeh, J. Chen, 18.1: invited paper: flexibility improvement of foldable AMOLED with touch panel, *SID, Symp. Dig. Tech. Papers* 46 (1) (2015) 238–241 <https://doi.org/10.1002/sdtp.10445>.
- [7] S.M. Lee, J.H. Kwon, S. Kwon, K.C. Choi, A review of flexible OLEDs toward highly durable unusual displays, *IEEE Trans. Electron. Dev.* 64(5)(2017)1922–1931 <https://doi.org/10.1109/ted.2017.2647964>.
- [8] Y. Obata, S. Kawabata, H. Kawai, Mechanical properties of natural rubber vulcanizates in finite deformation, *J. Polym. Sci.* 8 (6) (1970) 903–919 <https://doi.org/10.1002/pol.1970.160080607>.
- [9] Yeh M K, Chang L Y, Cheng H C, et al. Bending stress analysis of laminated foldable touch panel [J]. *Procedia Engineering*, 2014, 79: 189-193.
- [10] Yongzhen Jia, Zhengzhou Liu, Di Wu, Jifeng Chen, Hong Meng. Mechanical simulation of foldable AMOLED panel with a module structure [J]. *Organic Electronics*, 2019, 65: 185-192.

Table 1. The simplified 7-layer display film stack layout and the properties used in the simulation. The thickness shown in the table are the values used for stack layout 2

Panel Component	Thickness	Elasticity Modulus (GPa)	Poisson ratio
Cover Window	90	5.6	0.29
OCA1	50	/	0.48
Polarizer	47	3.769	0.33
OCA2	20	/	0.5
Touch	25	2.3	0.31
OCA3	25	/	0.49
TFE	9	76.9	0.22
Array	7.5	49	0.30
PI Substrate	15	9.1	0.33
OCA4	25	/	0.5
PET Backplane	75	4.076	0.32

Table 2 Prony coefficient g_i for different E_{∞}

Elastic Modulus	C_{10}	C_{20}	C_{30}	D_1
E	0.01061	-0.00012	1.7318×10^{-6}	4.79455
10E	0.10611	-0.00121	1.7318×10^{-5}	0.47946
100E	1.06053	-0.01206	1.7318×10^{-4}	0.04795
1000E	10.6053	-0.12057	1.7318×10^{-3}	0.00480
10000E	106.053	-1.20570	1.7318×10^{-2}	0.00048

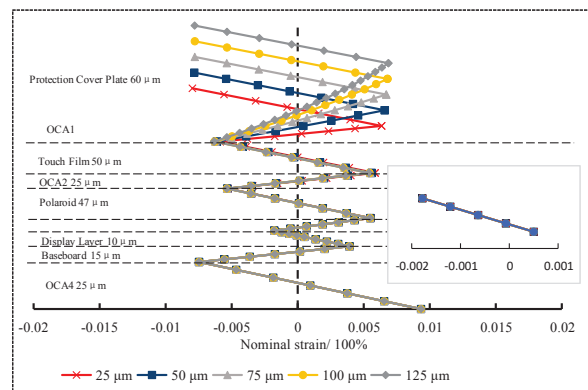


Fig3-1(a) The strain at the symmetry axis

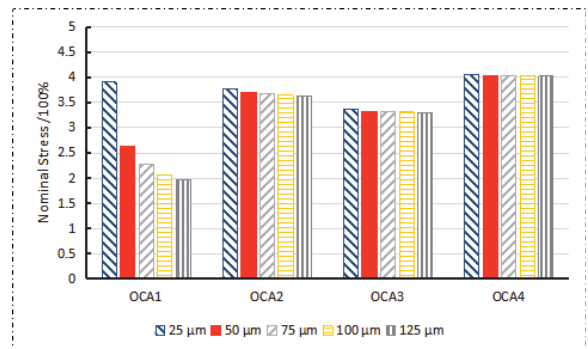


Fig3-1(b) The maximum strain of each OCA layer axis

Fig3-1 Comparison of different thickness OCA1 adhesive layers after bending

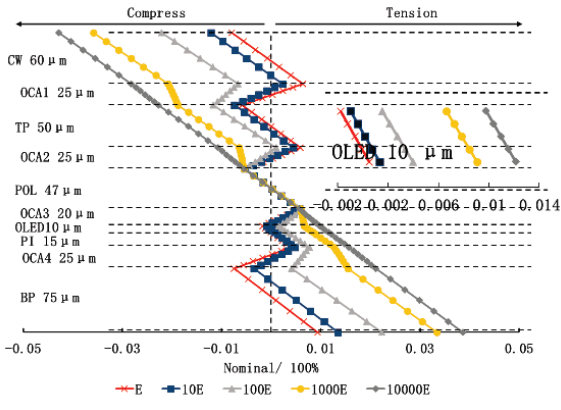


Fig3-2(a) The strain at the symmetry axis

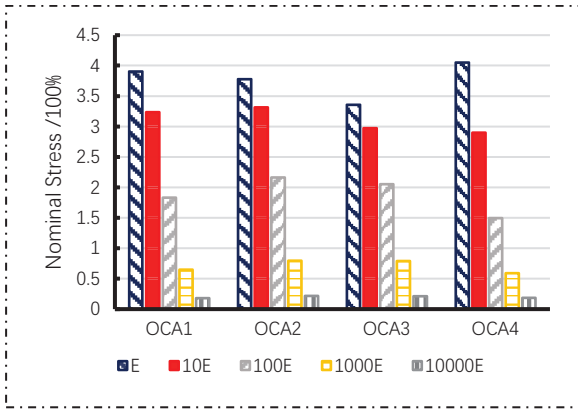
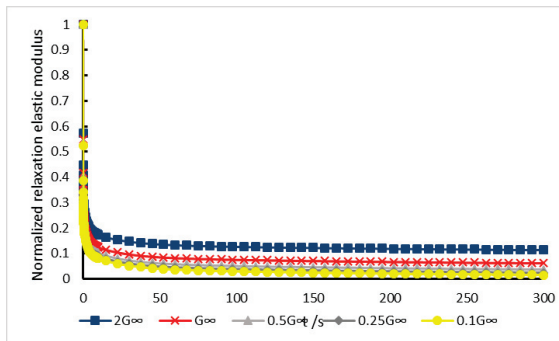
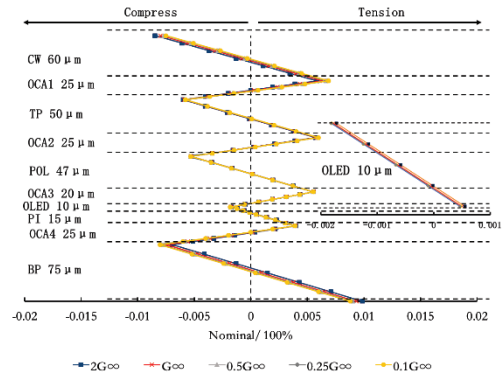


Fig3-2(b) The maximum strain of each OCA layer axis

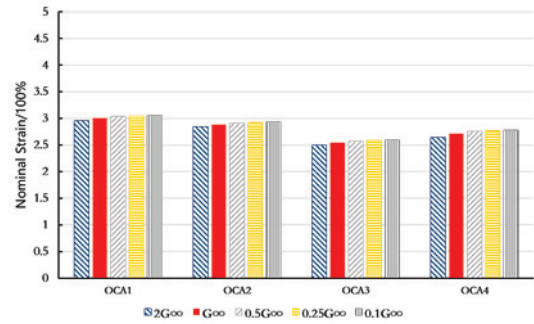
Fig3-2 Comparison of different elastic modulus after bending



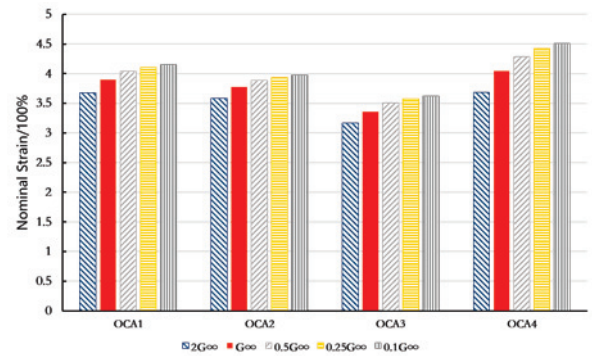
(a) The strain at the symmetry axis



(b) The maximum strain of each OCA layer axis



(c) Maximum strain of each rubber layer at 0 s



(d) Maximum strain of each rubber layer at 300 s

Fig3-3 Comparison of different viscoelastic E_∞ after bending